Flow Angle Effects on Supersonic Flutter of Curved Panels

Mohamed Salim Azzouz and Idir Azouz
Midwestern State University
salim.azzouz@mwsu.edu,

Abstract

A frequency domain non linear Finite Element formulation (FE) is presented herein to investigate the effects of arbitrary flow angle on the flutter structural response of isotropic curved skin panels under supersonic flow. The first-order shear deformation theory, the Marguerre curved plate theory, the von Karman strain-displacement relations, and the quasi-steady first order piston theory appended with a static aerodynamic load (SAL) are used as the backbones of the nonlinear finite element formulation. The triangular Mindlin (MIN3) plate element with improved shear correction factor is used in the developed source code. The principle of virtual work is applied herein to develop the equations of motion of the fluttering simply supported curved panel in structural node degrees of freedom (DOF) and the Newton-Raphson iteration method is employed to determine the static aerodynamic deflection and the dynamic flutter equation. The curved panel stiffness and deflection shape are accurately determined under the SAL for a specific range of dynamic pressure and yaw flow angles. In this paper the Flutter stability boundaries for different yaw flow angles and specific panel height rises are thoroughly investigated using the frequency coalescence analysis.

Introduction

Panel flutter is considered one of the major structural issues for high speed airplanes and aerospace vehicles. The surface skin panel under yawed supersonic flow may experience a sudden structural fatigue failure resulting in the loss of the vehicle. The determination of the flutter stability boundaries under the aforementioned conditions is essential to avoid such losses. The present paper focuses on the determination of the critical dynamic pressure of curved panels under a yawed supersonic flow.

In the sixties and early seventies researchers have investigated the effect of yawing flows on the flutter stability boundaries of isotropic and orthotropic flat rectangular panels at supersonic speeds. Several review articles devoted sections to the influence of yaw flow angle [1, 2] on panel flutter. Little literature has been dedicated to their effects on curved panels. A brief and quick review of yawing flow effects on the flutter of flat isotropic and composite plates will be instructive and inspiring for the present work. Kordes and Noll [3], and Bohon [4] studied analytically the influence of yawing flow angles on flutter of isotropic and composite rectangular panels with simply supported boundary conditions.

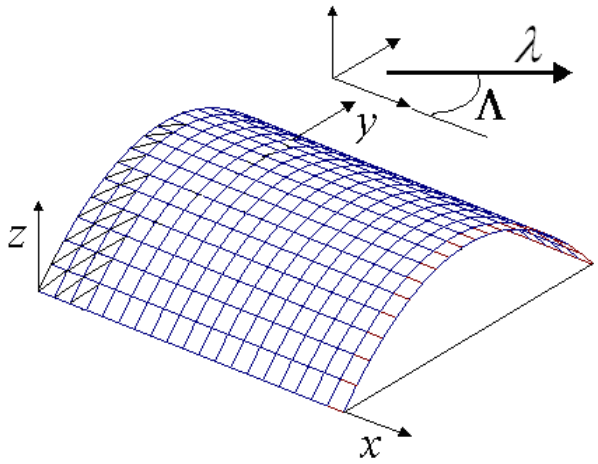

Fig. 1 Curved panel geometry with dynamic pressure λ and yaw flow angle Λ

Using the Raleigh-Ritz method appended with a 16-term trigonometric beam function, Dursasula [5] studied the plate obliquity effect on an isotropic rectangular plate subjected to a flow yawing for simply supported and clamped boundary conditions. Kari-Appa et al. [6], and Sander et al. [7] used the finite element method to study the effect of flow yawing of isotropic parallelogram panels. Shyprykevich and Sawyer [8], and Sawyer [9] have shown experimentally and theoretically that critical dynamic pressure is intimately related to the nature of the boundary conditions and the yaw flow angle. They demonstrated that orthotropic panels mounted on flexible support experienced large reduction in critical dynamic pressure for only small changes of flow angles. Additional developments on the linear finite element method applied to the aeroelastic stability of plates and shells under supersonic flow were reported by Bismarck-Nasr [1].

An extensive search of the open literature reveals that few investigations on non-linear panel flutter have considered the effects of flow yawing. Friedmann and Hanin [10] used first order piston theory and PDE/Galerkin method to investigate non-linear flutter under yawed supersonic flow. They solved the reduced coupled non-linear ordinary differential modal equations with numerical integration using a four by two (4x2) mode model in vacuo, four natural modes in the x direction, and two modes in the y direction. They obtained limit cycles for simply supported isotropic and orthotropic rectangular panels. Chandiramani et al, [11] used third order piston theory in conjunction with PDE/Galerkin method. They solved the reduced coupled non-linear ordinary differential modal equations using a predictor and a Newton-Raphson type corrector technique for limit-cycle periodic solutions. They employed direct numerical integration for non-periodic and chaotic solutions and used a two by two (2x2) mode model, two natural modes in the x direction and two natural modes in the y direction for simply supported rectangular laminated panels. Recently Abdel-Motagaly et al. [12] presented a finite element formulation with an efficient solution procedure for analysis of supersonic non-linear flutter of composite panels with arbitrary flow direction. The finite element non-linear panel flutter equations were first formulated in the structural-node degrees of freedom (DOF). The number of equations was reduced using a modal transformation. The minimum number of linear natural modes needed for an accurate and

convergent limit cycle flutter response was accurately determined. The reduced non-linear modal equations were solved using the linearized update mode with non-linear time function (NTF/LUM). Isotropic and composite panels at yawed supersonic flow were treated. They showed that yaw flow angle significantly affects the critical dynamic pressure and the limit cycle deflection.

The flutter of curved panels under arbitrary yaw flow angle received little attention until recently. Pidaparti and Yang [13] were the only team who investigated a linear flutter structural analysis of laminated composite plates and shells using finite elements. Their aerodynamic load did not account for the SAL. They demonstrated that the critical dynamic pressure versus yaw flow angle has a maximum for cylindrical panels with cross-stream curvature; whereas for spherical panels the relationship is increasing monotonically. Recently, a time domain and a frequency domain non-linear flutter structural analysis of curved panels with a formulation considering an arbitrary yaw flow angle was presented by the first author [14, 15].

In the present paper a frequency domain non-linear finite element formulation using the extended triangular Mindlin (MIN3) element in conjunction with the first-order shear deformation theory, the Marguerre curved plate theory, the von Karman strain-displacement relations, and the quasi-steady first order piston theory appended with a static aerodynamic load (SAL). The principle of virtual work is then applied to determine the equations of motion of the fluttering simply supported curved panel in structural node degrees of freedom (DOF) and the Newton-Raphson iteration method is used to determine the static aerodynamic deflection and the dynamic flutter equation. The critical dynamic pressure for different flow angle configurations is determined by the equation of motion eigen solutions.

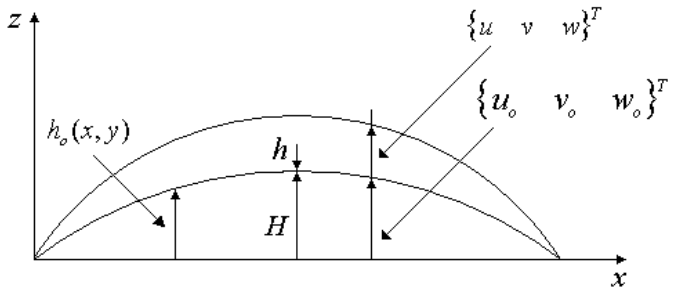

Fig. 2 Curved panel geometry characterized by the height-rise H/h

Finite Element Formulation: Constitutive Equations

The simply supported curved panel when exposed to flutter experiences large deflections, therefore the total strain vector is composed of the inplane linear and nonlinear strain components according to the von Karman large deflection theory, the strain due to curvature according to Marguerre shallow shell theory, and strain due to bending

$$\{\varepsilon\} = \begin{Bmatrix} \varepsilon_x \\ \varepsilon_y \\ \gamma_{xy} \end{Bmatrix} = \begin{Bmatrix} u_{,x} \\ v_{,y} \\ u_{,y} + v_{,x} \end{Bmatrix} + \frac{1}{2}\begin{Bmatrix} w_{,x}^2 \\ w_{,y}^2 \\ 2w_{,x}w_{,y} \end{Bmatrix} + \begin{Bmatrix} w_{,x}h_{o,x} \\ w_{,y}h_{o,y} \\ w_{,x}h_{o,y} + w_{,y}h_{o,x} \end{Bmatrix} + \bar{z}\begin{Bmatrix} \psi_{y,x} \\ \psi_{x,y} \\ \psi_{y,y} + \psi_{x,x} \end{Bmatrix}$$

$$= \{\varepsilon_m^o\} + \{\varepsilon_b^o\} + \{\varepsilon_h^o\} + z\{\kappa\} = \{\varepsilon^o\} + z\{\kappa\} \tag{1}$$

and the transverse shear strains are

$$\{\gamma\} = \begin{Bmatrix} \gamma_{yz} \\ \gamma_{xz} \end{Bmatrix} = \begin{Bmatrix} w_{,y} \\ w_{,x} \end{Bmatrix} + \begin{Bmatrix} \psi_x \\ \psi_y \end{Bmatrix} \tag{2}$$

The subscripts b, h, and m stand for bending, curvature, and membrane strain components. Considering the general case of a composite laminate curved panel, the normal stresses are expressed for the kth layer as

$$\{\sigma\}_k = \begin{Bmatrix} \sigma_x \\ \sigma_y \\ \tau_{xy} \end{Bmatrix}_k = \begin{bmatrix} \overline{Q}_{11} & \overline{Q}_{12} & \overline{Q}_{16} \\ \overline{Q}_{12} & \overline{Q}_{22} & \overline{Q}_{26} \\ \overline{Q}_{16} & \overline{Q}_{26} & \overline{Q}_{66} \end{bmatrix}_k \begin{Bmatrix} \varepsilon_x \\ \varepsilon_y \\ \gamma_{xy} \end{Bmatrix} = \left[\overline{Q}\right]_k \{\varepsilon\} \tag{3}$$

and the shear stresses for the kth layer are expressed as

$$\{\tau\}_k = \begin{Bmatrix} \tau_{yz} \\ \tau_{xz} \end{Bmatrix}_y = \begin{bmatrix} \overline{Q}_{44} & \overline{Q}_{45} \\ \overline{Q}_{45} & \overline{Q}_{55} \end{bmatrix}_k \begin{Bmatrix} \gamma_{yz} \\ \gamma_{xz} \end{Bmatrix} = \left[\overline{Q}_s\right]_k \{\gamma\} \tag{4}$$

The constitutive equations for the composite curved panel laminate are

$$\begin{Bmatrix} N \\ M \end{Bmatrix} = \begin{bmatrix} [A] & [B] \\ [B] & [D] \end{bmatrix} \begin{Bmatrix} \varepsilon^o \\ \kappa \end{Bmatrix}, \text{ and } \{R\} = [A_s]\{\gamma\} \tag{5}$$

The quasi-steady first order piston theory is employed herein for the aerodynamic pressure load over the curved skin panel and is expressed according to Ashley and Zartarian [16] as

$$p - p_\infty = -\frac{2q_a}{\beta}\left(\{w_{,x}\}\cos\Lambda + \{w_{,y}\}\sin\Lambda\right) - \frac{2q_a}{\beta}\left(\frac{M_\infty^2 - 2}{M_\infty^2 - 1}\frac{1}{V_\infty}\{w_{,t}\}\right) - \frac{2q_a}{\beta}\left(h_{o,x}\cos\Lambda + h_{o,y}\sin\Lambda\right) \tag{6}$$

The effect of the flow angle has been added to Eq. (6). The term $q_a = \rho_a V_\infty^2/2$ is the dynamic pressure and $\beta = \sqrt{M_\infty^2 - 1}$ is the Prandtl-Glauert factor. The symbol Λ is the arbitrary yaw flow angle with respect to x axis, Fig 1, and $h_{o,x}$ and $h_{o,y}$ are the derivatives with respect to x

and y of the curved panel geometry $h_o(x, y)$. Applying the principle of virtual work and proceeding with the assembly process, the system equations of motion in structure-nodes DOF after applying the kinematic boundary conditions are

$$\frac{1}{\omega_o^2}[M]\{\ddot{W}\}+\frac{g_a}{\omega_o}[G]\{\dot{W}\}+\left([A_a]+[K_L]+\frac{1}{2}[N1]+\frac{1}{3}[N2]\right)\{W\}=\{P_s\} \quad (7)$$

where

$$[A_a]=\lambda\cos\Lambda[A_x]+\lambda\sin\Lambda[A_y] \quad (8)$$

is the total aerodynamic stiffness matrix,

$$[K_L]=[K]+[K]^s+[K_o]^{\theta_o} \quad (9)$$

is the total linear stiffness matrix,

$$[N1]=[N1]^{\theta}+[N1]^{\theta_o}+[N1]^{N_b}+[N1]^{N_m}+[N1]^{N_{\theta_o}} \quad (10)$$

is the total first-order stiffness matrix,

$$[N2]=[N2]_{\theta}^{\theta} \quad (11)$$

is the second-order stiffness matrix

and

$$\{P_s\}=-\lambda\cos\Lambda\{P_{h_{o,x}}\}-\lambda\sin\Lambda\{P_{h_{o,y}}\} \quad (12)$$

is the static aerodynamic load.

The matrix $[M]$ represents the system mass matrix, $[G]$ the system aerodynamic damping, $[A_x]$ the system aerodynamic stiffness matrix with respect to x direction, $[A_y]$ the system aerodynamic stiffness matrix with respect to y direction, $[K]$ the system linear stiffness matrix, $[K]^s$ the system linear shear stiffness matrix, $[K_o]^{\theta_o}$ the system linear stiffness matrix due to the shallow shell geometry including a single geometrical matrix $[\theta_o]$, $[N1]^{\theta}$ the system non-linear first-order stiffness matrix, $[N1]^{\theta_o}$ the system non-linear first-order stiffness matrix due to shallow shell geometry, $[N1]^{N_b}$ the system non-linear first-order stiffness matrix due to the nodal vector $\{w_b\}$, $[N1]^{N_m}$ the system non-linear first-order stiffness matrix due to the nodal vector $\{w_m\}$, $[N1]^{N_{\theta_o}}$ the system non-linear stiffness matrix due to the shallow shell geometry and the nodal vectors $\{w_b\}$ and $\{w_\psi\}$, $[N2]_{\theta}^{\theta}$ the system non-linear second-order stiffness matrix, $\{P_{h_o}\}$ is the static aerodynamic loads, and $\{W\}$ is

the system nodal displacement vector. The geometrical curved matrix $[\theta_o]$ is a function of the derivatives of the curved panel geometry $h_o(x, y)$ as

$$[\theta_o] = \begin{bmatrix} h_{o,x} & 0 \\ 0 & h_{o,y} \\ h_{o,y} & h_{o,x} \end{bmatrix} \tag{13}$$

The parameters λ and g_a in Equation (7) and (8) refer to the non-dimensional dynamic pressure and the aerodynamic damping, respectively, and are

$$\lambda = \frac{2q_a a^3}{\beta D_{110}}, \text{ and } g_a = \sqrt{\lambda C_a} \tag{14}$$

where,

$$C_a = \frac{\mu\left(M_\infty^2 - 2\right)^2}{\beta\left(M_\infty^2 - 1\right)^2}, \text{ with } \mu = \frac{\rho_a a}{\rho h} \tag{15}$$

for $M_\infty >> 1$, $C_a \approx \frac{\mu}{M_\infty}$.

The parameter $\omega_o = \left(D_{110}/\rho h a^4\right)^{1/2}$ is a reference frequency, and D_{110} is the first entry in laminate bending rigidity $[D]$ for a unidirectional zero degree laminate.

According to Gray, [17], the solution of an ordinary differential system of equations with a steady state load term can be separated as a time-independent particular solution and a time-dependent homogenous solution. Therefore the total panel deflection can be separated as

$$\{W\} = \{W\}_s + \{W(t)\}_t \tag{16}$$

The homogenous solution characterizes a self-exited dynamic oscillation $\{W(t)\}_t$, while the particular solution characterizes an aerodynamic static equilibrium deflection $\{W\}_s$. Substituting Equation (16) into (7), the equation of motion can be separated into two distinctive equations as

$$\frac{1}{\omega_o^2}[M]\{\ddot{W}(t)\}_t + \frac{g_a}{\omega_o}[G]\{\dot{W}(t)\} + \left([A_a] + [K_L] + \frac{1}{2}[N1]_t + \frac{1}{3}[N2]_t \right)\{W(t)\}_t$$
$$+ \left(\frac{1}{2}[N1]_t + \frac{1}{3}[N2]_t + \frac{2}{3}[N2]_{st} \right)\{W\}_s + \left(\frac{1}{2}[N1]_s + \frac{1}{3}[N2]_s + \frac{2}{3}[N2]_{st} \right)\{W(t)\}_t = \{0\}$$

(17)

and

$$\left([A_a] + [K_L] + \frac{1}{2}[N1]_s + \frac{1}{3}[N2]_s \right) \{W\}_s = \{P_s\} \tag{18}$$

Equation (18) is a set of non-linear algebraic equations. The equation solution $\{W_s\}$ is an aerostatic deflection under a specific SAL $\{P_s\}$ at a prescribed dynamic pressure λ. The subscripts *s*, *t*, *st* refer to that the non-linear stiffness matrices $[N1]_s$, $[N1]_t$, $[N2]_t$, $[N2]_s$, and $[N2]_{st}$ are evaluated with $\{W\}_s$ or $\{W(t)\}_t$, or both simultaneously.

Eigen Problem Formulation

Neglecting the inplane inertia term in Eq. (7), the in-plane displacement vector $\{W^m\}$ can be rewritten as a function of the bending and rotational displacement vector $\{W^b\}$.

$$\{W^m\} = -[K_m]^{-1}[K_B^T]\{W^b\} - [K_m]^{-1}[K_B^{\theta_o^T}]\{W^b\} - \frac{1}{2}[K_m]^{-1}[N1_{mb}]\{W^b\} \tag{19}$$

The system equations (7) are then expressed in terms of the bending and rotational displacement vector as

$$\frac{1}{\omega_o^2}[M]^b\{\ddot{W}^b\} + \frac{g_a}{\omega_o}[G]^b\{\dot{W}^b\} + \left([A_a]^b + [K_L]^b + [K1]^b + [K2]^b\right)\{W^b\} = \{P_{sal}^b\} \tag{20}$$

where the aerodynamic stiffness matrices is given by

$$[A_a]^b = \lambda\cos\Lambda[A_x] + \lambda\sin\Lambda[A_y] \tag{21}$$

the linear stiffness matrices are given by

$$[K_L]^b = [K_b] + [K_s] + [K_b^{\theta_o}] - [K_B][K_m]^{-1}[K_B^T] - [K_B][K_m]^{-1}[K_B^{\theta_o^T}] - [K_B^{\theta_o}][K_m]^{-1}[K_B^T] - [K_B^{\theta_o}][K_m]^{-1}[K_B^{\theta_o^T}] \tag{22}$$

The non-linear stiffness matrices are given by

$$[K1]^b = \frac{1}{2}[N1_b] + \frac{1}{2}\left[N1_b^{\theta_o}\right] + \frac{1}{2}\left[N1^{N_b}\right] + \frac{1}{2}\left[N1^{N_m}\right] + \frac{1}{2}\left[N1^{N_{\theta_o}}\right] - \frac{1}{2}[N1_{bm}][K_m]^{-1}\left[K_B^T\right]$$
$$-\frac{1}{2}[K_B][K_m]^{-1}[N1_{mb}] - \frac{1}{2}\left[K_B^{\theta_o}\right][K_m]^{-1}[N1_{mb}] - \frac{1}{2}[N1_{bm}][K_m]^{-1}\left[K_B^{\theta_o^T}\right] \quad (23)$$

and

$$[K2]^b = +\frac{1}{3}[N2_b] - \frac{1}{4}[N1_{bm}][K_m]^{-1}[N1_{mb}] \quad (24)$$

the load vector is given by

$$\left\{P_{sal}^b\right\} = \left\{P_{sal}^b\right\} \quad (25)$$

The solution to the eigenvalue problem of Eq. (20), can be assumed as an exponential time function

$$\left\{W^b\right\} = \{\phi\}e^{\Omega t} = \{\phi\}e^{(\alpha+i\omega)t} \quad (26)$$

Where the non-dimensional eigenvalue κ is defined as

$$\kappa = -\left(\frac{\Omega^2}{\omega_o^2}\right) - g_a\frac{\Omega}{\omega_o} \quad (27)$$

The eigen-solution of Eq. (20) has a very specific and unique set of eigen-values and eigen-vectors fingerprinting exclusively the particular geometry of the curved panel.

Results and Discussion

An aluminum 3-dimensional isotropic cylindrical panel of dimensions a×b×h (12.0×12.0×0.04 in., 30.48×30.48 ×0.1016 cm) with simply supported edges along the x direction and the y directions is investigated for flutter critical dynamic pressure λ at different yaw flow angles Λ, Fig.1. The material density is ρ = 0.00025234 lb×s^2/in.^{4} (2700 kg/m^3), the modulus of elasticity is E = 5×10^6 psi (7.1×10^{10} Pa) and the Poisson ratio ν = 0.3. Immovable in-plane edges u(0, y) = u(a, y) = v(x, 0) = v(x, b) = 0 are considered herein. The cylindrical panel is modeled with 16×16 mesh size representing 512 MIN3 elements, Tessler and Hughes [18]. The number of structure DOF is 735 for the curved skin panel system after applying the boundary conditions.

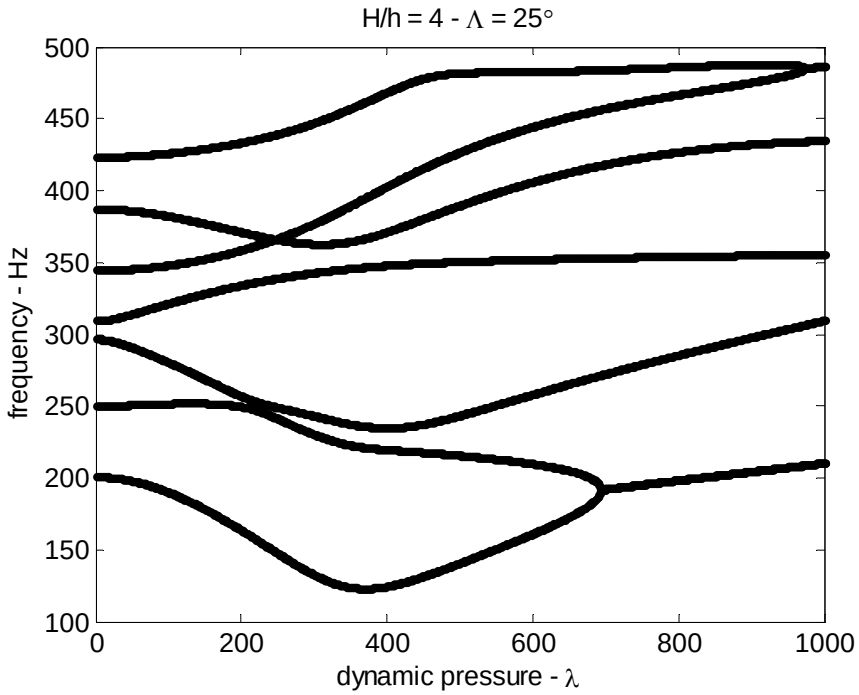

Fig. 3 Flutter coalescence curve of a 3-D simply supported cylindrical panel with a height-rise of H/h = 4 and yaw flow angle of Λ=25°

The different curves in Fig. 3 represent the evolution of the frequencies associated with the aerostatic modes, [15], function of the dynamic pressure with a particular flow angle. Each curve is associated with one aerostatic mode. As an example the lowest curve denominated herein curve 1 is associated with the aerostatic mode 1, curve 2 is associated with the aerostatic mode 2, and so on. It can be noted from the figure that as the frequencies associated with the aerostatic modes evolve with higher dynamic pressure a frequency coalescence process is taking place. When the coalescence occurs the curved skin panel experience an instability status called flutter. The dynamic pressure at which flutter occurs is called critical dynamic pressure. As an example in here the critical dynamic pressure corresponding to the coalescence of the frequencies associated with aerostatic modes 1 and 2 is λ_{cr} = 694. It is interesting to notice that a gradual softening of the frequency associated with aerostatic mode 1 then a hardening occurs till the coalescence point, whereas the frequency associated with aerostatic mode 2 experiences a relative softening toward the coalescence point. This softening process may lead to a sudden buckling of the panel, [19].

The bell curve in Fig. 4 represents the progression of the critical dynamic pressure λ_{cr} function of the yaw flow angle Λ for a cylindrical curved panel with height rise of H/h = 1.it is very important to notice that all dynamic pressure above the bell curve represent a region of flutter instability. it is also worthwhile to notice in this particular case that all the frequency coalescence corresponding to the critical dynamic pressure called also in the literature flutter onset occur between the frequencies corresponding to aerostatic mode 1 and aerostatic mode 2 without exception. Herein the height rise of the panel is very small and of

the order of the thickness H/h = 1. The curved panel in this case is assimilated to a near plate system, in other words behaves dynamically more or less like a flat plate system. It is remarkable to notice also from Fig. 4 that the highest critical dynamic pressure occur at a yaw flow angle of $\Lambda = 45°$. This fact is of prime importance, it tells the aircraft manufacturer that there is a preferential panel orientation to maximize the flutter stability boundaries for this particular near plate panel.

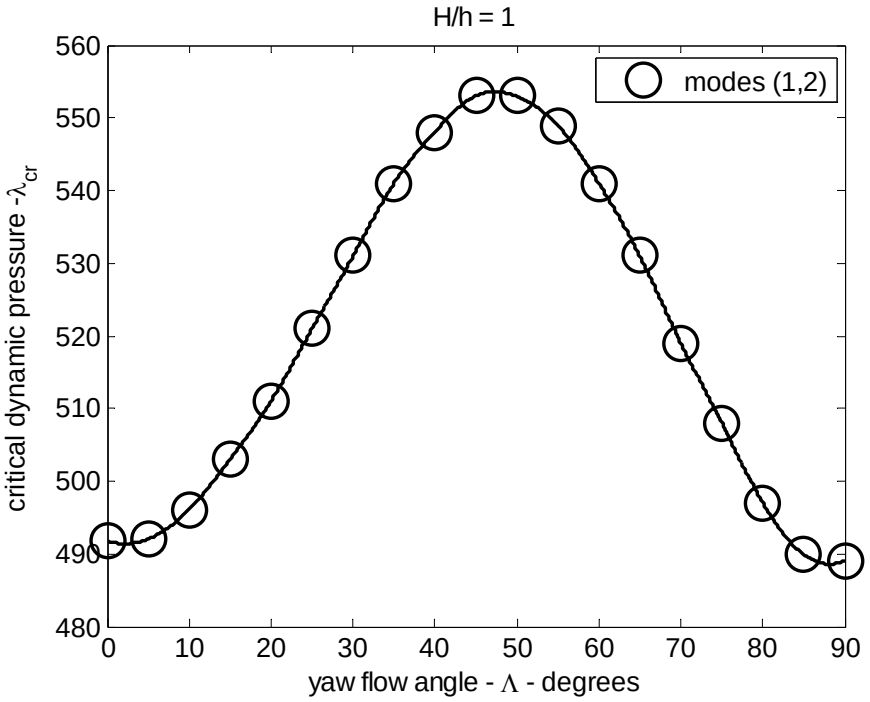

Fig. 4 Flutter critical dynamic pressure function of the yaw flow angle for a 3-D simply supported cylindrical panel with a height rise of H/h = 1

By increasing the curved panel height rise to two times the thickness H/h = 2, it is seen from Fig. 5 that an increase of the curvature is beneficial to the cylindrical panel for a yaw flow angle in the range of $0° \leq \Lambda < 75°$. For this particular yaw flow angle range all the critical dynamic pressure are the results of the frequency coalescence between aerostatic mode 1 and aerostatic mode 2. The critical dynamic pressure increase seen in Fig. 5 enhances the panel resistance to flutter by bringing the flutter stability boundaries upward. This fact is clearly noticeable when comparing the highest critical dynamic pressure for panels with height rise H/h =1, $\lambda_{cr} = 553$, and panels with an increased height rise H/h = 2, $\lambda_{cr} = 754$. Unfortunately, for yaw flow angles between $75° < \Lambda < 90°$ the panel experiences a sudden decrease in the flutter stability boundaries. Herein, the flutter onset is due to the coalescence of the frequencies associated to aerostatic modes 2 and aerostatic mode 3. The coalescence of aerostatic mode 2 and aerostatic 3 occurs at a much lower dynamic pressure, $\lambda_{cr} = 385$. We can say in this case that for the range of yaw flow angles $75° < \Lambda < 90°$, the curvature is detrimental with respect to the flutter stability boundaries.

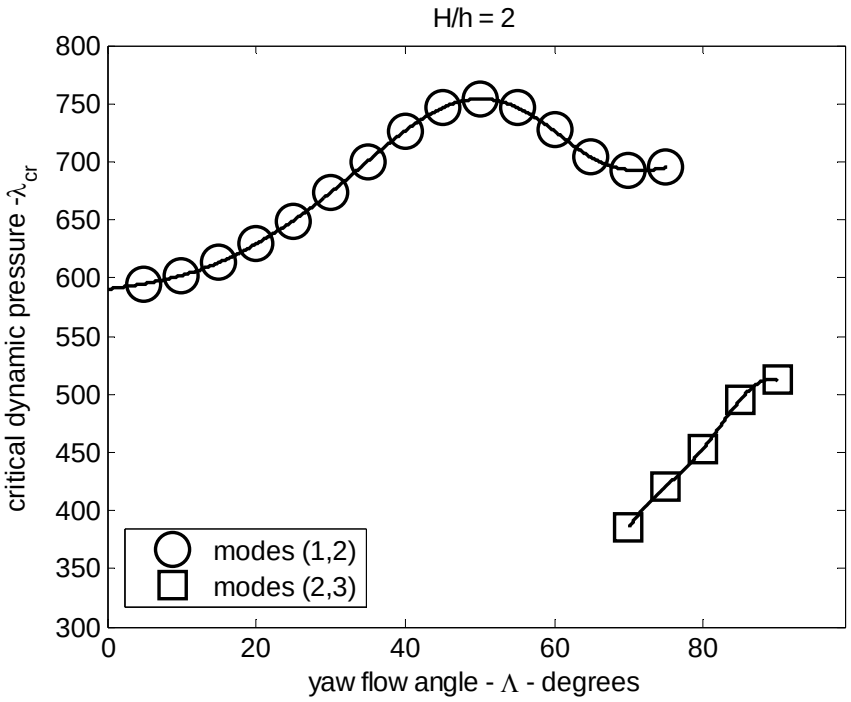

Fig. 5 Flutter critical dynamic pressure function of the yaw flow angle for a 3-D simply supported cylindrical panel with a height rise of H/h = 2

Increasing further the height rise to H/h = 3, Fig 6, it can be noticed that the flutter stability boundaries are pushed further upward for a yaw flow angles range of $0° < \Lambda < 70°$. A decrease of 5° in the beneficial yaw flow range with respect to the panel yaw flow range with a height rise of H/h = 2. Notice that the maximum critical dynamic pressure $\lambda_{cr} = 944$ occurs at $\Lambda = 56°$ an increase of 25.2 % with respect to the previous panel, H/h = 2. The sudden drop in the critical dynamic pressure occurs in the neighborhood of the yaw flow angle of $\Lambda = 70°$, and the critical dynamic pressure decreases to $\lambda_{cr} = 396$. Notice that this critical dynamic pressure increased slightly with respect to the one corresponding to the panel height rise H/h = 2. The increase is only 2.85 %. It is also worthwhile to notice that in the yaw flow range of $70° < \Lambda < 90°$, the critical dynamic pressure is essentially due to the coalescence of the frequencies corresponding to aerostatic mode 2 and aerostatic mode 3.

Conclusion

From the present study, it can be concluded that for a near plate curved panel of height rise of H/h = 1, there is a preferential panel orientation to maximize the critical dynamic pressure. For curved panels with a height rise of H/h = 2, and 3, the effect of curvature on the flutter stability boundaries is beneficial for a certain low and medium range of yaw flow angles and detrimental for a higher yaw flow angles range.

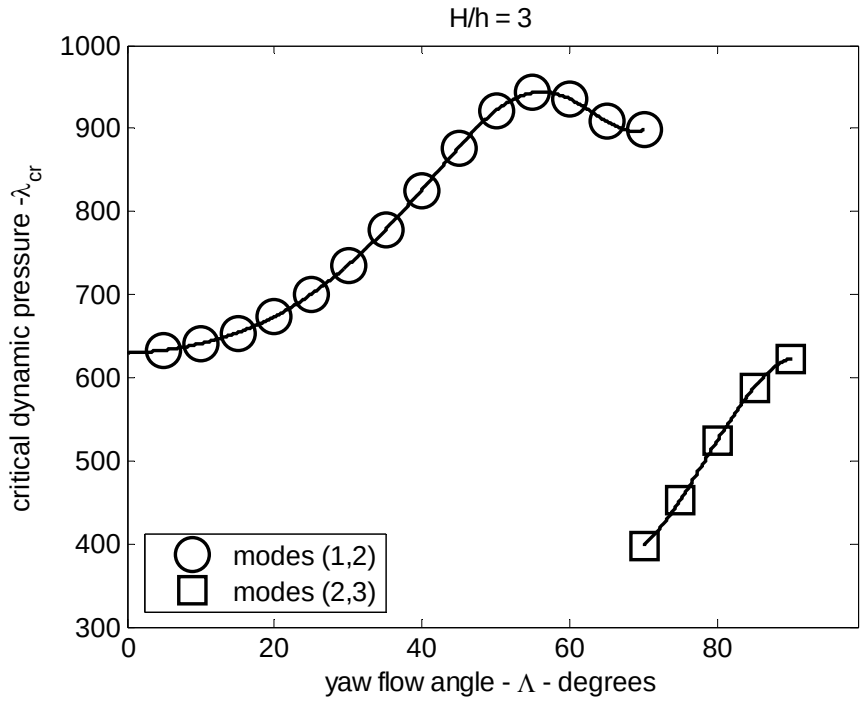

Fig. 6 Flutter critical dynamic pressure function of the yaw flow angle for a 3-D simply supported cylindrical panel with a height rise of H/h = 3

References

[1] Bismarck-Nasr, M. N., "Finite Element Analysis of Aeroelasticity of Plates and Shells," Applies Mechanics Review, Vol. 45, No. 12, Part 1, 1992, pp. 461-482.

[2] Mei, C., Abdel-Motagaly, K., and Chen, R., "Review of Non-linear Panel Flutter at Supersonic and Hypersonic Speeds," Applied Mechanic Review, Vol. 52, No. 10, October 1999, pp. 321-332.

[3] Kordes, E. E., and Noll, R. B., "Theoretical Flutter Analysis of Flat Rectangular Panels in Uniform Coplanar Flow with Arbitrary Direction," NASA TN D-1156, 1962.

[4] Bohon, H. L., "Flutter of Flat Rectangular Orthotropic Panels with Biaxial Loading and Arbitrary Flow Direction," NASA TN D-1949, 1963.

[5] Dursasula, S., "Flutter of Clamped Skew Panels in Supersonic Flow," Journal of Aircraft, Vol. 8, No. 6, 1971, pp. 461-466.

[6] Kari-Appa, V., Somashekar, B. R., and Shah, C. G., "Discrete Element Approach to Flutter of Skew Panels with In-plane Forces Under Yawed Supersonic Flow," AIAA Journal, Vol. 8, No. 11, 1970, pp. 2017-2022.

[7] Sanders, G., Bon, B., and Geradin, M., "Finite Element Analysis of Supersonic Panel Flutter," International Journal for Numerical Methods in Engineering, Vol. 7, No. 3, 1973, pp. 379-394.

[8] Shyprykevich, P., and Sawyer, J. W., "Orthotropic Panel Flutter at Arbitrary Yaw Angles-Experiment and Correlation with Theory," AIAA Paper 73-192, 11th Aerospace Sciences Meeting, January 1973, Washington, DC.
[9] Sawyer, J. W., "Flutter of Elastically Supported Orthotropic Panels Including the Effects of Flow Angle," NASA TN D-7491, 1974.
[10] Friedmann, P., and Hanin, M., "Supersonic Non-linear Flutter of Orthotropic or Isotropic Panels with Arbitrary Flow Direction," Israel Journal of Technology, Vol. 6, No. 1-2, 1968, pp. 46-47.
[11] Chandiramani, N. K., Plaut, R. H., and Librescu, L., "Nonperiodic Flutter of Buckled Composite Panel," Sadhana Journal, Vol. 20, No. 2-4, 1995, pp. 671-689.
[12] Abdel-Motagaly, K., Chen, R., and Mei, C., "Non-linear Flutter of Composite Panels Under Yawed Supersonic Flow Using Finite Elements," AIAA Journal, Vol. 37, No.9, September 1999, pp. 1025-1032.
[13] Pidaparti, R. M. V., and Yang, H. T. Y., "Supersonic Flutter Analysis of Composite Plates and Shells," AIAA Journal Vol. 31, No. 6, June 1993, pp. 1109-1117.
[14] Azzouz, M., S., Przekop, A., Guo, X., And Mei, C., "Nonlinear Flutter of Shallow Shell Under Yawed Supersonic Flow Using FEM," AIAA 2003-1516, 44th SDM Conference, Norfolk, VA, April 2003.
[15] Azzouz, M. S., Guo, X., Przekop, A. and Mei, C., "Nonlinear Flutter of Cylindrical Shell Panels Under Yawed Supersonic Flow Using FE," AIAA 2004-2043, 45th SDM Conference, Palm Spring, CA, April 2004.
[16] Ashley, H., and Zartarian, G., "Piston Theory – A New Aerodynamic Tool for the Aeroelastician," Journal of Aeronautical Science, Vol. 23, No. 10, 1956, pp. 1109-1118.
[17] Gray, C. C., "Finite Element Analysis of Thermal Post-Buckling and Vibrations of Thermally Buckled Composite Plates," Msc. Thesis, Aerospace Department, Old Dominion University, March 1991.
[18] Tessler, A. and Hughes, T. J. R., "A Three-node Mindlin Plate Element With Improved Transverse Shear," Computer Methods in Applied Mechanics and Engineering, Vol. 50, 1985, pp. 71-91.
[19] Azzouz, M. S., "Nonlinear Flutter of Curved Panels Under Yawed Supersonic Flow Using Finite Elements," Ph.D. Dissertation, Department of Aerospace Engineering, Old Dominion University, January 2005.

Biography

MOHAMED SALIM AZZOUZ is currently an Assistant Professor at the McCoy School of Engineering at Midwestern State University (MSU), Wichita Falls, Texas. Dr. Azzouz has over 8 years of industry experience as an engineer, and 4 year as an educator. He worked with a subsidiary of the group Dannon in Switzerland and the group Siemens in the state of Virginia.

IDIR AZOUZ is a professor of engineering and chair of the McCoy School of Engineering at Midwestern State University (MSU). He earned a Ph.D. in mechanical engineering from Tulsa University and focused his research on turbulent flow of drag-reducing fluids. His contribution to this field includes several peer-reviewed publications.